Time Variability Patterns of Eutrophication Indicators in the Bay of Algeciras (South Spain)

Jesús M. Mercado [1,*] **, Pablo León** [1,2] **, Soluna Salles** [1] **, Dolores Cortés** [1] **, Lidia Yebra** [1] **, Francisco Gómez-Jakobsen** [1] **, Inma Herrera** [1] **, Aitor Alonso** [1] **, Antonio Sánchez** [1] **, Nerea Valcárcel-Pérez** [1] **and Sébastien Putzeys** [1]

[1] Instituto Español de Oceanografía, Centro Oceanográfico de Málaga, Puerto Pesquero s/n, 29640 Fuengirola, Málaga, Spain; pablo.diaz@gov.scot (P.L.); solunasalles@uma.es (S.S.); lcortes@ieo.es (D.C.); lidia.yebra@ieo.es (L.Y.); fgomez.jakobsen@ieo.es (F.G.-J.); inma_herri@hotmail.com (I.H.); zaszum@hotmail.com (A.A.); antoniosanchezysanchez@gmail.com (A.S.); nerea.valcarcel@ieo.es (N.V.-P.); sputzeys@gmail.com (S.P.)

[2] Present address: Marine Scotland Science, Marine Laboratory, 375 Victoria Road, Aberdeen AB119DB, UK

[*] Correspondence: jesus.mercado@ieo.es

Abstract: In the Bay of Algeciras (BA), intensive urban and industrial activityis underway, which is potentially responsible for the release of significant quantities of nutrients. However, the assessment of the impact of these discharges is complex. Nutrient concentration in the surface layer is *per se* strongly variable due to the variability associated with the upwelling of nutrient-enriched deep Mediterranean water (MW), which in turn is regulated by atmospheric forcing. The aim of this study is to determine the effects of changes in the upwelling intensity on the load of nitrate and phosphate in the BA and to appraise their impact on chlorophyll *a* variability. Based on this analysis, the possible influence of the nutrients released from land-based sources is indirectly inferred. Data and samples collected during nine research cruises carried out in different seasonal cycle periods between 2010 and 2015 in the BA were analysed. The vertical variation of temperature and salinity indicates that the MW upwelling was favoured in spring, as occurred in other coastal areas of the northern Alboran Sea. However, principal component analysis conducted on physical and chemical data reveals that shifts in nutrients and chlorophyll *a* in the euphotic layer are poorly explained by changes in the upwelling intensity. Furthermore, during some of these research surveys (particularly in summer), chlorophyll *a* concentrations were higher in the BA as compared to a nearby coastal area also affected by MW upwelling. Scarce information about land-based pollution sources precludes quantitative analysis of the impact of nutrient loads on water quality; however, the available data suggest that the main source of allochthanous inorganic nitrogen over the period 2010–2015 in the BA was nitrate. Therefore, it is reasonable to hypothesize that the high concentrations of nitrate and chlorophyll *a* in BA in summer are a consequence of those discharges. Our study highlights the need of more exhaustive inventories of sewage and river discharges to adequately rate their impact in the BA.

Keywords: nitrate; phosphate; chlorophyll *a*; phytoplankton; upwelling; sewage; eutrophication assessment

1. Introduction

Coastal eutrophication is considered a process by which symptoms are progressive, with multiple effects on the marine ecosystems. In the first phase, nutrient pollution is shown by increases in chlorophyll *a* concentrations in the water column and/or opportunistic macroalgae abundance; subsequently, changes in the phytoplankton community composition, including increased frequency

of unpleasant and potentially toxigenic blooms and a decrease in dissolved oxygen concentration, are produced [1,2]. According to this conceptual scheme, eutrophication assessment in a given system requires knowledge of how external sources impact the nutrient budget in the water column as well as the relationships between nutrient excess and phytoplankton abundance and composition. For many coastal areas, the application of this evaluation scheme is challenging due to the association of nutrient natural variability with vertical displacements of water masses, and the complexity of the relationships between nutrient concentration and chlorophyll *a* (normally used as a proxy of phytoplankton biomass [3]). Thus, while concomitant increases of nutrient concentration and chlorophyll *a* have been reported in multiple marine systems [4,5], an increase in nutrient load did not result in increasing trends of phytoplankton biomass in some other cases [6,7]. Furthermore, increases in chlorophyll *a* concentration have been reported in a few systems during periods of nutrient load reduction [5,8,9]. According to Cloern [4], this variety of responses is due to the physical and/or biological attributes of each particular system which act as filters by modulating the effects of nutrient enrichment. These filters include tidal energy [10], optical properties of the water column [4], and horizontal transport processes dependent on wind, bathymetry, basin geography, and river flows. Furthermore, Li et al. [11] reported that the response of chlorophyll *a* to changing nutrients would vary according to the time scale considered. For instance, in some systems studied by Li et al. [11], short-term (diel and intra-annual) and decadal variability in chlorophyll *a* was attributable to changes in nitrate concentration, while interannual chlorophyll *a* variability was apparently not related to nutrients. These findings suggest that the mechanisms underlying the nutrient-driven phytoplankton dynamics could differ not only across different coastal systems but also even within a particular system, depending on the time scale.

The Bay of Algeciras (BA) is a suitable case study to illustrate the difficulties in assessing nutrient pollution effects in coastal areas. This semi-enclosed bay is situated in the northern coast of the Alboran Sea (the westernmost basin in the Mediterranean Sea), close to the Strait of Gibraltar (the confluence of the Atlantic Ocean and the Mediterranean Sea; Figure 1). With an area of approximately 73 km^2 and a maximum depth of 400 m, the BA supports some of the most intense maritime traffic in Europe, channelled towards the harbours of Algeciras (which is ranked among the most important ports of the world) and Gibraltar. The bay is influenced by freshwater input from two rivers (Palmones and Guadarranque) and sewage discharge from intensive industrial activity (a stainless steel manufacturing plant, petrochemical and petroleum refineries, paper mills, thermal power plants, shipyards) and urban areas (with a total population of almost 300,000 inhabitants). Agriculture and livestock activity around the BA is fairly reduced. Consequently, the release of nutrients from non-point sources must be also reduced compared to industrial and urban inputs.

As occurs in most of the northern coast of the Alboran Sea, the water column in the BA is normally occupied by two water masses, the surface Atlantic Water (SAW) and deep Mediterranean Water (MW). According to Periáñez [12] and Sánchez-Garrido [13], the horizontal circulation patterns in BA are mainly regulated by the Atlantic Jet (AJ) entering the Alboran Sea through the Strait of Gibraltar. Changes in the position of the AJ with respect to the northern shoreline, due to atmospheric forcing, modify the circulation modes inside BA [14]. On the other hand, the wind regime regulates the amount of SAW and MW in the BA and affects the ascension of MW towards the euphotic layer. According to Sánchez-Garrido et al. [13], easterly winds fill the bay with SAW, while westerlies drain it. Additionally, tidal currents appear to be the main mechanisms regulating the flushing times of SAW, while the flushing times of the Mediterranean layer are less variable and do not depend on tides. According to these authors' calculations, the flushing time of the whole BA water ranges from 10 to 20 days. A recent study based on a Lagrangian model for surface particle dispersion [14] supports that renewal times are fairly variable among different areas within the BA depending on wind conditions.

The studies published on contaminant dispersion and their effects in the BA have focused on sediment [15,16] and benthic communities [17,18]. Periáñez [12] calculated that the horizontal transport of contaminants that tend to form aggregated with settling suspended particles inside the

BA is relatively weak. Consequently, the plumes of these contaminants which originate from different terrestrial sources stay close to the pollution point. It is worth noting that Carballo et al. [19] concluded that the benthic community composition within the BA was affected by urban and industrial waste. However, there are no studies specifically aimed at determining soluble nutrient dispersion within the BA and its effects on the phytoplankton communities.

The vertical mixing of the water column promoted by the upwelling of MW, with a higher nutrient concentration in comparison to SAW, would be expected to produce the nutrient enrichment of the euphotic layer. Therefore, productivity in the BA should be linked to water mass movements that favour this natural enrichment mechanism, as has been described for other coastal areas in the Alboran Sea [20,21]. In contrast, if phytoplankton growth is fuelled by land-based nutrient sources, changes in chlorophyll *a* concentration would not fit the hydrodynamic variability patterns. The aims of this study are: (1) to assess the effects of changes in MW upwelling intensity on the load of nitrate and phosphate in the BA; and (2) to appraise the impact of this variability on chlorophyll *a*. The potential impact of eutrophication on the BA is examined by inferring indirectly the possible influence of the nutrient release from land-based sources.

2. Materials and Methods

2.1. Study Area and Hydrographical Profiles.

The BA was the target of nine oceanographic cruises carried out between 2010 and 2015 on board the research vessels Francisco de Paula Navarro and R/V Emma Bardán. Samplings were carried out in the framework of the projects *Estrategia Marina: Eutrofizacion* (3-ESMAREU and 2-3 ESMAREU) as part of a monitoring program specifically aimed to assess eutrophication in the Spanish Mediterranean Coast. Data and samples were collected at four sampling stations located along a north–south transect within BA (Figure 1). The geographical location of the stations was based on a thorough analysis of a time series of chlorophyll *a* satellite images for the period 2002–2010 (data not shown). This strategy allowed us to cover adequately the chlorophyll *a* gradient observed in the BA, normally located from the northern coast to the centre of the bay, and to avoid the influence of coastal structures (ports and docks), which modify the surface circulation pattern at a small scale [14]. Additionally, three stations located close to the BA in the northern Alboran Sea (Sotogrande; ST) in Figure 1) were sampled one day after visiting the BA. ST stations, with depths of 10, 15, and 65 m, were located in a transect perpendicular to the coast. Survey dates allowed sampling events to cover the three main phases of the seasonal cycle previously identified in the northern Alboran Sea [20,21] (Table 1): the bloom period (from late winter to April), the stratification period (summer, from June to September); and the destratification period (autumn). Note that the exact date of each survey was constrained by the research vessel availability and/or the meteorological conditions.

Table 1. Sampling dates and stations in the Bay of Algeciras.

| Survey	Year	Data	Seasonal Period	Stations
EU0710 (10/07)	2010	11 July	Stratification	AG1, AG2, AG3
EU1111 (11/11)	2011	25 November	Destratification	AG1, AG2, AG3, AG4
EU0312 (12/03)	2012	8 March	Bloom	AG1, AG2, AG3
EU0712 (12/07)	2012	14 July	Stratification	AG1, AG2, AG3, AG4
EU1112 (12/12)	2012	30 November	Destratification	AG1, AG2, AG3, AG4
EU0414 (14/04)	2014	19 April	Bloom	AG1, AG2, AG3, AG4
EU0614 (14/06)	2014	3 June	Stratification	AG1, AG2, AG3, AG4
EU1114 (14/11)	2014	27 October	Destratification	AG1, AG2, AG3, AG4
EU0415 (15/04)	2015	21 April	Bloom	AG1, AG2, AG3, AG4
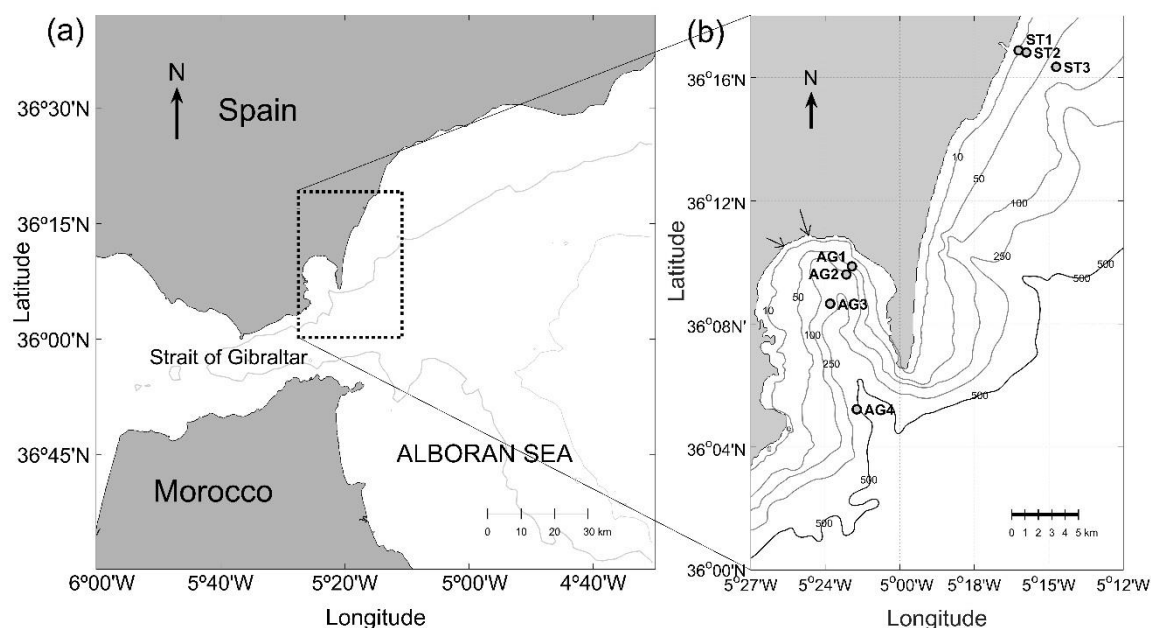
Figure 1. Area of study (panel **a**) and location of sampling stations in the Bay of Algeciras (stations AG1–AG4) and Sotogrande (ST1–ST3). Thin black arrows in panel (**b**), indicate the position of the mouths of the two main rivers (Palmones and Guadarranque) within the Bay.

Vertical profiles of temperature, salinity and chlorophyll *a* fluorescence at every meter were obtained at each station with a CTD Seabird 25 (Sea-Bird Scientific, Belleuve, WA, USA) equipped with a fluorescence probe (Seapoint 6000, Seapoint Sensor Inc., Exeter, NH, USA) and a photosynthetically active radiation (PAR) spherical probe (Biospherical-LICOR, Biospherical Instrument Inc., San Diego, CA, USA). The euphotic layer depth (ELD) was estimated from the descending profiles of PAR as the depth at which 1% of surface irradiance was reached. Mixed layer depth (MLD) was calculated according with the method proposed by Kara et al. [22], as the depth at which the potential density changed by 0.5 compared with the surface reference value. This threshold has shown the best results to determine the proper pycnocline in previous studies performed in the northern Alboran Sea [20,23].

Data on the annual nutrient load discharged by industrial and urban effluents from 2010 to 2015 towards the coastal waters of the north-western Alboran Sea were gathered from the Environmental Information Net of the Andalusian Ministry of Environment (REDIAM; www.juntadeandalucia.es/ medioambiente/rediam). The amount of dissolved inorganic nitrogen (ammonium plus nitrate) and phosphate input from the two main rivers that discharge into the BA (the Palmones and Guadarranque rivers) was estimated from the nutrient concentrations measured close to their mouths (data available at http://laboratoriorediam.cica.es/Visor_DMA from the Andalusian Ministry of Environment). These nutrient concentrations were multiplied by the figures of caudal flow averaged annually published in [24]. Data of annual load of nitrogen released from non-point sources were also obtained from [24].

2.2. Sampling Strategy and Analysis Procedures

In both sampling areas (i.e., BA and ST), water samples were collected with Niskin bottles at different fixed depths (0, 10, 20, 30, 40, and 100 m or near the bottom when shallower). At a minimum, four depths were sampled in the shallow station (st. 1) and a maximum of six in the rest (st. 2, 3 and 4) in the BA. Sub-samples of 10 mL of seawater were collected from each bottle and immediately frozen at $-20\,^\circ$C for nutrient analysis. The concentration of nitrite plus nitrate, nitrite, phosphate and silicate were determined using a segmented flow analyser (Bran-Luebbe AA3, SPX Flow Technology Norderstedt GmbH, Norderstedt, Germany), following the methods described in

Ramírez et al. [25]. Chlorophyll *a* concentration was determined in samples filtered through fiber glass filters (Whatman GF/F, GE Healthcare UK Limited, Little Chalfont, Buckinghamshire, UK) measuring 0.7 μm in pore diameter (total chlorophyll; Chl_T *a*). Additional samples were filtered through 20-μm pore polycarbonate filters in order to discriminate chlorophyll by larger size fraction of phytoplankton ($Chl_{>20}$ *a*). Volumes of 1 and 2 L of seawater were used for Chl_T *a* and $Chl_{>20}$ *a*, respectively. Filters were immediately frozen at −20°C until their analysis in the laboratory. The analysis of chlorophyll *a* was conducted by spectrophotometry, after extraction in 90% acetone overnight at 4–5 °C. Between 1–2 L of sample was collected for determination of particulate organic nitrogen (PON) and carbon (POC). The samples were screened using a 200-μm retention mesh and subsequently filtered onto precombusted (450 °C for 2 h) Whatman GF/F filters previously dried at 60 °C. The filters were stored frozen until being exposed to HCl fumes overnight in the lab. The organic matter content in the filters was analysed with a Perkin-Elmer 2004 CNH elemental analyser (Perkin-Elmer, Madrid, Spain) after burning in an oven (LECOVTF 900, LECO Corporation, Saint Joseph, MI, USA).

Additional water samples were collected in the BA stations to analyse the abundance of diatoms, dinoflagellates and autotrophic flagellates. Samples were fixed in dark glass bottles with Lugol's solution (2% final concentration). In the laboratory, 100 mL of each fixed sample were allowed to settle in a composite chamber for 24 h, following the technique developed by Utermöhl. Cells were counted at 200× and 600× magnification with a Leica DMIL inverted microscope (Leica Microsistemas, L'Hospitalet de Llobregat, Spain). For all the stations, samples collected at surface and at the chlorophyll *a* maximum depth were analysed using this method. These data are shown as Supplementary material (Figure S1) since the phytoplankton results corresponding to 2012/12 and 2014/06 are not available.

2.3. Statistical Analysis

In order to assess the seasonal variability patterns in the BA, means of the different variables obtained within the euphotic layer in the four stations were calculated for each survey. For these calculations, only data on temperature and salinity (which were sampled every meter) coinciding with the nutrient sampling depths were considered. These means were used to calculate averaged values for bloom (surveys 2012/03, 2014/04, 2015/04), stratification (surveys 2010/07, 2012/07 and 2014/06) and destratification periods (surveys 2011/11, 2012/11 and 2014/11). Pearson's correlation analyses between some variables were performed. The main variability patterns of nutrients and chlorophyll *a* and their relationships with temperature and salinity were assessed with principal component analysis [26]. The statistical analyses were carried out with the software package Statistica 7.1 (Statsoft, Inc. 1984–2005, Tulsa, OK, USA).

3. Results

3.1. Temperature and Salinity

Across all survey years and seasons, salinity and temperature ranged from 36.5 to 38.3 and 13.3 °C to 22.2 °C, respectively. The maximum salinity range at the surface for the water quality monitoring cruises occurred during the 2014/11 and 2014/04 sampling events (36.5–37.3). For each cruise, temperature and salinity profiles were fairly similar in the four sampling stations. However, significant variability was observed among surveys carried out during the same phase of the seasonal cycle (Figures 2 and 3). For instance, during the stratification period (summer surveys) strong gradients in temperature and salinity were obtained in the upper 20 m in 2010/07 and 2014/06, while these gradients were located below 50 m in depth in 2012/07. Similarly, the spring samplings showed a shallower density gradient in 2014/04 compared to 2012/03 and 2015/04. Concordantly, the MLD was fairly variable, although the lower limit of the mixed layer was located in the upper 40–50 m depth in all stations, apart from some stations sampled during the annual destratification period (2011/11 and 2014/11). On the other hand, the mixed layer was restricted to the upper 25-m layer during 2010/07 and 2014/04.
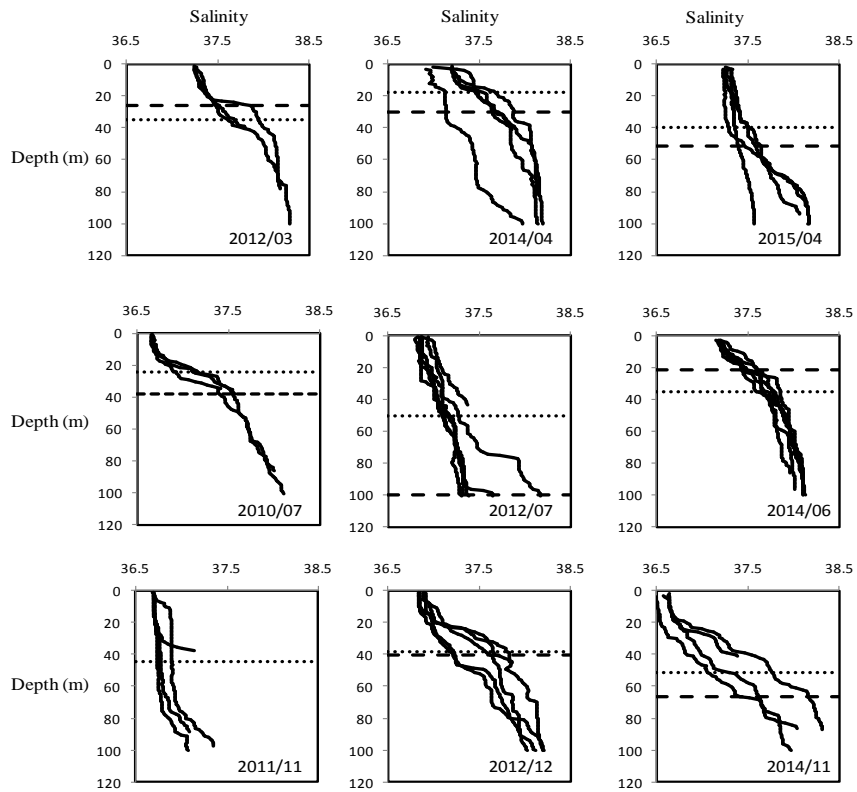
Figure 2. Vertical profiles of salinity obtained in the sampling stations in the Bay of Algeciras during the research surveys carried out from 2010 to 2015. The lower limit of mixed layer (fine dotted line) and the average position of the Mediterranean–Atlantic interface (AMI depth; thick dashed line) for each research survey are shown. Plots are grouped according to three seasonal periods: spring (**top**), summer (**middle**), and autumn (**bottom**).
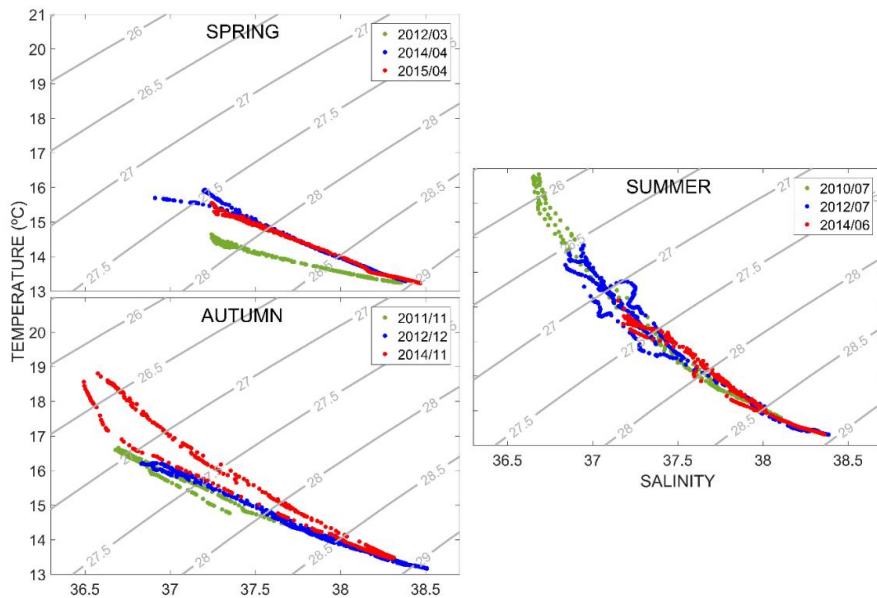

Figure 3. Temperature-salinity plots obtained during the different research surveys. The data are grouped according to three seasonal periods: spring (**top left**), summer (**middle**), and autumn (**bottom left**).

The analysis of the T-S diagrams reveals that the water column was occupied by the mixing of two water masses in all sampling stations (Figure 3). The first mass corresponds to warmer and fresher water (salinity 36.6–36.7) that characterises the SAW; with salinity values between 38.4 and 38.5 and temperature values around 13 °C; the other water mass corresponded with Intermediate Levantine Water, that is MW. In the Alboran Sea (see references cited in the Introduction), the 37.5 isohaline is considered to indicate the position of the interface between SAW and MW (AMI). Figure 2 shows that the AMI depth averaged for each research survey varied substantially. In fact, it was located at an approximately 100-m depth in 2012/07 and deeper in the four stations sampled during 2011/11. The AMI was located in the upper 30 m in 2012/03 and 2014/06.

3.2. Vertical Profiles of Nutrients, Chlorophyll a and Particulate Matter

In all stations, nitrate concentrations in the surface layer were lower as compared to the 100-m depth (Figure 4). Higher nitrate concentrations (ca. 8 μM) were obtained in samples collected below an 80-m depth. In contrast, nitrate concentration was lower than 0.6 μM in most samples collected at surface, being under the detection limit (0.04 μM) in some samples collected during 2011/11, 2012/07, 2012/12, 2014/06 and 2015/04. At that depth level, nitrate concentrations higher than 1 μM were only obtained during 2012/12 (note that the vertical distribution of nitrate during this survey was fairly uniform in comparison to the other surveys). The nitrite concentration was below 0.25 μM in all samples with the exception of some collected during 2010/07 below a 20-m depth, which presented concentrations above 0.65 μM. Overall, nitrite concentration in the water column showed low variability throughout the study.

Silicate and phosphate variability patterns were similar to those obtained for nitrate (see Figure 4 for phosphate; data for silicate are not shown). However, in contrast to nitrate, the higher phosphate concentrations (above 0.4 μM) in the whole water column were obtained during 2015/04 and 2014/11. In agreement with these differences in nitrate and phosphate among depths and surveys, the molar ratio of nitrate+nitrite to phosphate (N:P) was fairly variable, ranging from less than 5 (obtained in multiple samples collected at surface) to 45 (obtained in station 2 during 2012/03; Figure 5). In general, N:P increased with depth, apart from 2012/12 and 2015/04 when the profiles were homogenous. In 2012/03 higher N:P ratios were obtained at intermediate depths. In most samples, N:P ratio was lower than 16:1; however, the N:P ratio exceeded this threshold in all samples collected in 2012/03 as well as in some samples collected below a 40-m depth in 2014/04, 2010/07, 2012/07 and 2014/06. The N:Si molar ratio followed similar variation patterns to those obtained for N:P (data not shown).
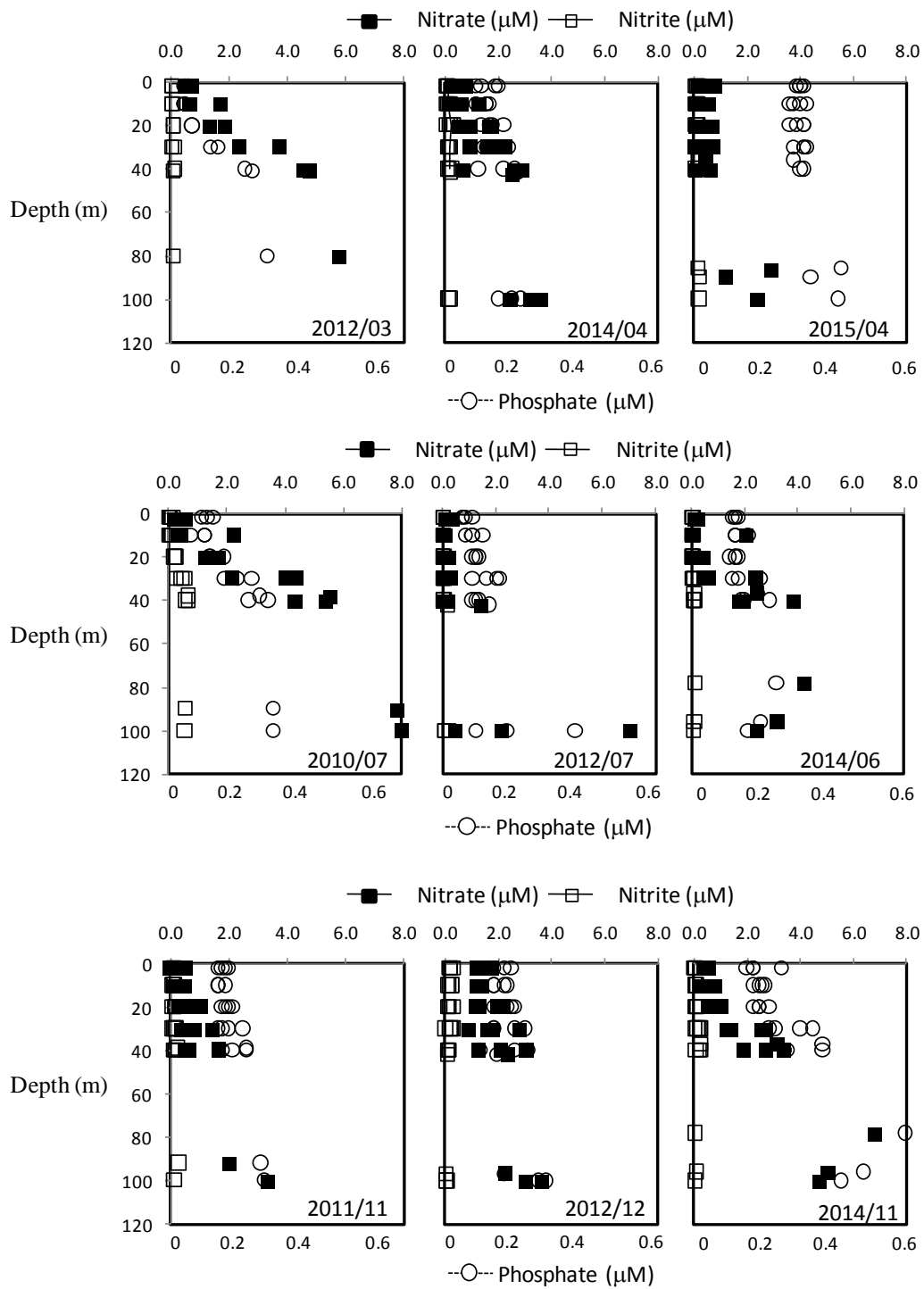
Figure 4. Variation along depth of nitrate, nitrite and phosphate concentrations obtained during surveys in the Bay of Algeciras. For each depth, the concentrations obtained in the four sampling stations are shown. Data were grouped according to three seasonal periods: spring (**top**), summer (**middle**), and autumn (**bottom**).
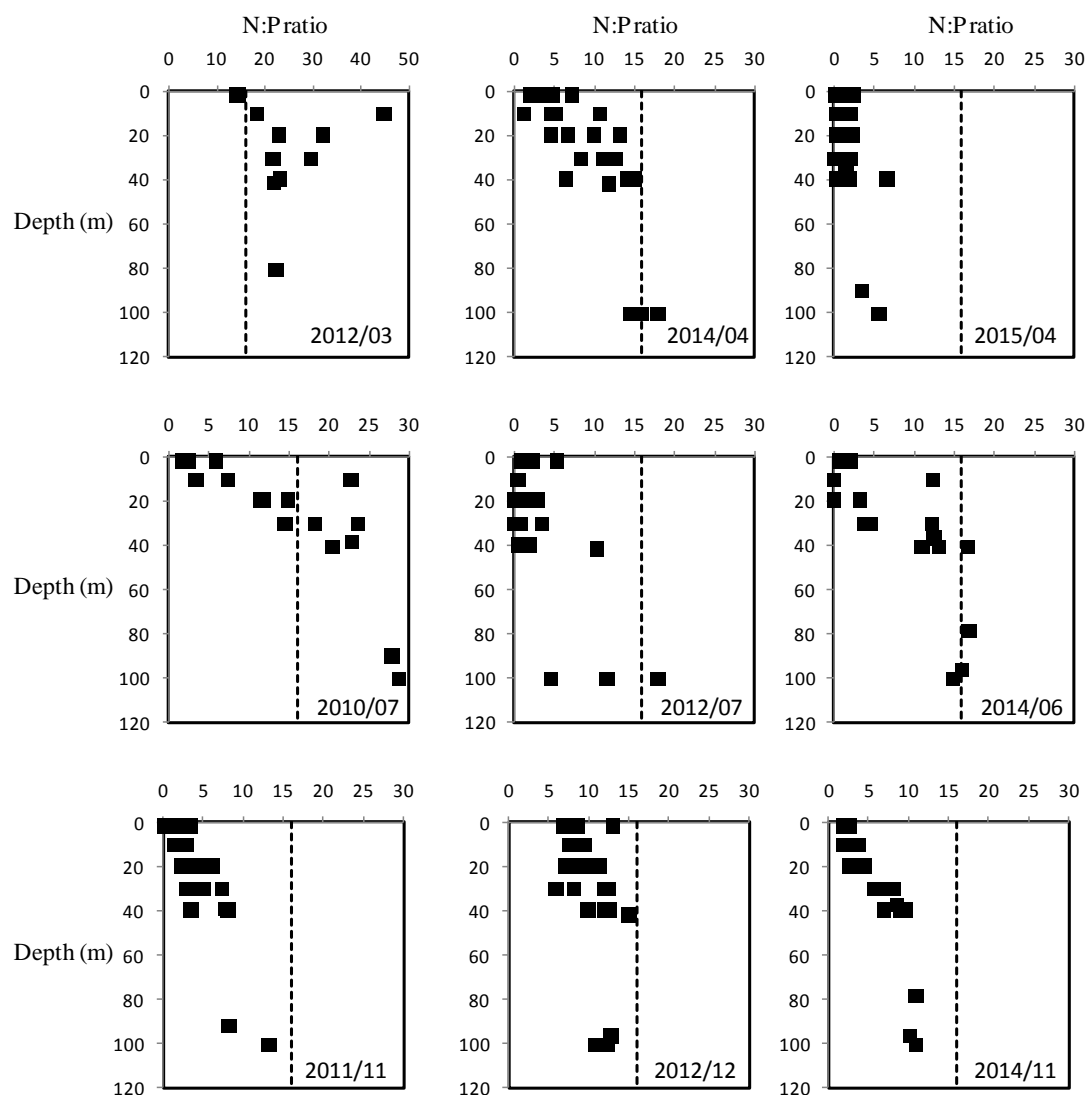
Figure 5. Variation along depth of the molar ratio nitrate+nitrite to phosphate (N:P) obtained during surveys in the Bay of Algeciras. For each depth, the N:P ratio obtained in the four sampling stations are shown. Vertical dashed lines indicate the Redfield ratio (16:1). Note the different *y*-axis scale for 2012/03. Data were grouped according to three seasonal periods: spring (**top**), summer (**middle**), and autumn (**bottom**).

Most chlorophyll *a* profiles collected during spring and summer showed a conspicuous sub-superficial maximum of both Chl_T *a* and $Chl_{>20}$ *a* (Figure 6). Within this maximum, higher Chl_T *a* (5–6 μg L^{-1}) concentrations were obtained during 2012/03 and 2014/06. The Chl_T *a* maximum obtained in 2012/03 was probably due to the high abundance of diatoms (702 cell mL^{-1}; although diatom abundance was also high in 2012/07; see Figure S1). In contrast, autumn chlorophyll *a* concentrations were comparatively higher at surface, except in 2014/11. In any case, concentrations of either Chl_T *a* and $Chl_{>20}$ *a* decreased substantially below a 40-m depth; significant concentrations of Chl_T *a* below this depth were only registered in station 3 during 2012/07. Concordantly, the lower limit of the euphotic layer was located in the upper 50-m depth, with the exception of station 3 during 2011/11. $Chl_{>20}$ *a* was strongly correlated to Chl_T *a* (*n* = 189; r^2 = 0.87; *p* < 0.001), suggesting that larger cells contributed uniformly to phytoplankton vertical and horizontal variability patterns. In fact, diatom abundance (with size ranges from 10 to 100 μm) was fairly reduced in 2010/07 and 2011/11 (less than 10 cell mL^{-1}; Figure S1) matching with fairly low $Chl_{>20}$ *a* concentrations.

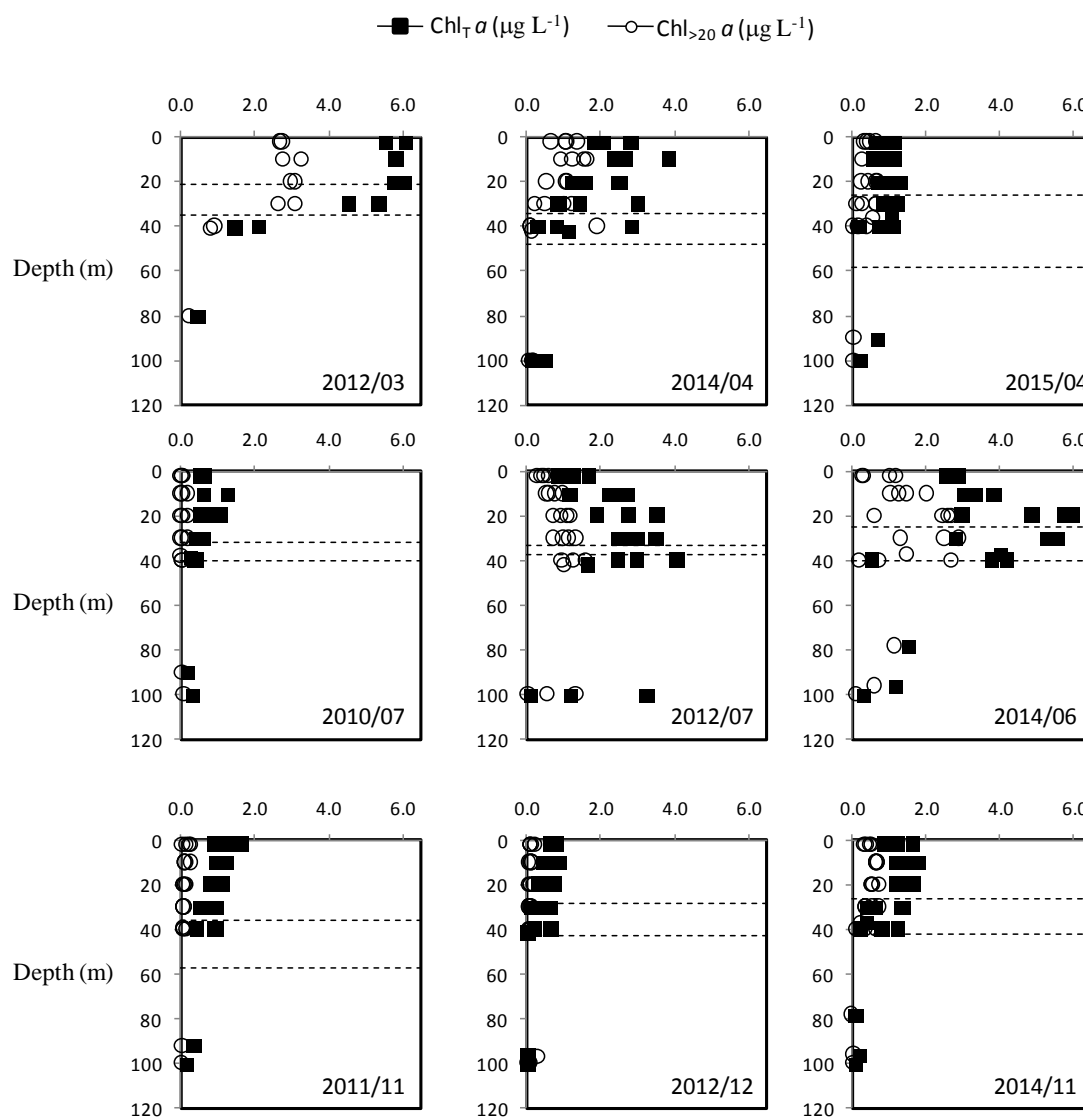**Figure 6.** Variation along depth of total and >20 μm chlorophyll *a* (Chl$_T$ *a*, fill symbols; Chl$_{>20}$ *a*, open symbols) obtained during surveys in the Bay of Algeciras. For each depth, Chl$_T$ *a* and Chl$_{>20}$ *a* values obtained in the four sampling stations are shown. The horizontal dashed lines show the variability range in the position of the euphotic layer lower limit. Data were grouped according to three seasonal periods: spring (**top**), summer (**middle**), and autumn (**bottom**).

POC and PON followed similar variation patterns to those obtained for Chl$_T$ *a* (data not shown); in fact, the correlations between POC and Chl$_T$ *a* ($n = 189$; $r^2 = 0.69$, $p < 0.001$) and PON and Chl$_T$ *a* ($n = 189$; $r^2 = 0.78$, $p < 0.001$) were statistically significant. These correlations indicate that the variability in particulate organic matter is mainly due to changes in phytoplankton biomass.

In comparison to the other area (ST) sampled during the surveys, salinity within the euphotic layer was slightly higher in BA but temperature showed similar values (Figure S2). Chl$_T$ *a* was higher in BA compared to ST in 2012/07 and 2014/06; while Chl$_T$ *a* in both areas was similar in 2010/07, coinciding with a much higher nitrate concentration in BA. It is worth noting that during this survey phytoplankton abundance and composition in BA was different to ST (data not shown). Thus, abundance of diatoms and flagellates in BA was 4.3 and 382 cell mL^{-1}, respectively. In contrast, diatoms were more abundant (13.2 cell mL^{-1}) in ST where flagellates reached only 185 cell mL^{-1}. Therefore, differences in nutrient concentrations between the two sampling areas were also reflected in variations of the phytoplankton community regardless of the Chl$_T$ *a* concentration.

3.3. Seasonal Variability

In spite of differences in the physical features of the water column among sampling stations within and among surveys, our data allow to discern some seasonal patterns. The SAW layer was more strongly modified by the mixing with MW in spring, as demonstrated by the higher surface salinity and lower temperature obtained during these surveys compared to summer and autumn (Table 2). Accordingly, on average, AMI was shallower in spring compared to autumn and summer. In contrast, the highest surface temperature was obtained in summer, as expected due to the seasonal warming cycle. Furthermore, on average the lowest surface salinity was obtained in autumn, probably indicating lower influence of MW on the surface water layer. It is worth noting that there were not differences in the MLD among the three seasonal periods.

Table 2. Seasonal mean $\pm$ standard deviation of the different variables estimated in the euphotic layer. Data correspond to the average value obtained during 2012/03, 2014/04 and 2015/04 for spring, 2010/07, 2012/07, and 2014/06 for summer, and 2011/11, 2012/11, and 2014/11 for autumn. AMI: Atlantic–Mediterranean interface depth; MLD: mixed layer depth; ELD: euphotic layer depth; Chl_T a, total chlorophyll a; POC and PON, particulate organic carbon and nitrogen, respectively.

	Spring	Summer	Autumn
Surface temperature (°C)	15.0 ± 0.8	17.8 ± 1.8	16.6 ± 0.5
Surface salinity	37.4 ± 0.3	37.0 ± 0.4	36.9 ± 0.2
Temperature (°C)	15.0 ± 0.5	17.5 ± 1.2	16.7 ± 1.1
Salinity	37.3 ± 0.1	37.1 ± 0.2	36.9 ± 0.2
AMI (m)	31.3 ± 18.7	75.4 ± 39.5	58.8 ± 32.5
MLD (m)	31.5 ± 16.9	34.3 ± 19.3	38.4 ± 20.1
ELD (m)	34.9 ± 10.1	39.3 ± 14.0	39.3 ± 8.9
Nitrate (µM)	0.87 ± 0.43	0.92 ± 1.03	1.03 ± 0.53
Phosphate (µM)	0.12 ± 0.13	0.12 ± 0.02	0.18 ± 0.03
Silicate (µM)	0.73 ± 0.11	0.96 ± 0.75	1.73 ± 0.61
N:P molar ratio	11.2 ± 12.0	5.4 ± 5.6	5.6 ± 3.3
N:Si molar ratio	1.2 ± 0.7	0.57 ± 0.35	0.63 ± 0.33
Si:P molar ratio	7.2 ± 5.5	7.8 ± 5.7	10.3 ± 5.0
Chl_T a (µg L^{-1})	3.0 ± 2.6	2.2 ± 1.5	0.95 ± 0.34
POC (µg L^{-1})	226 ± 139	237 ± 106	130 ± 27
PON (µg L^{-1})	30 ± 16	28 ± 12	20 ± 4

In order to assess if seasonal differences in the nutrient concentrations in the euphotic layer were correlated to changes in temperature and salinity, the average values of these variables were calculated for the three seasonal periods. The seasonal means were calculated by using all data obtained within the euphotic layer in the four stations sampled during the three surveys carried out in each seasonal cycle phase. The total numbers of samples used to these comparisons were 57, 48, and 54 for spring (bloom period), summer (stratification period), and autumn (destratification period), respectively. Nitrate concentration was similar in the three periods (Table 2). Phosphate and silicate concentrations were higher in autumn and N:Si molar ratio was significantly higher in spring. Chl_T a levels were also lower in autumn as well as POC and PON (note that the POC was higher in summer compared to spring).

To support the seasonal patterns distinguished above, a principal component analysis (PCA) was performed with physical (temperature and salinity) and chemical (nutrients, molar ratio of nutrients, Chl_T a and POC and PON) variables. Only the data collected within the euphotic layer were used to perform this analysis. The three first principal components (PC) extracted from the PCA explained more than 82% of the whole variability (Figure 7). Nitrate and silicate contributed positively to PC1, while Chl_T a and POC and PON did negatively. It is worth noting that the contribution of temperature and salinity to this PC was comparatively low. In contrast, these two variables contributed significantly to PC2. Consequently, it can be assessed that PC2 represents the main variability mode associated with

the seasonal changes in physical features of the water column. In fact, almost all samples collected during the autumn surveys presented negative scores for PC2 (i.e., lower salinity) while samples obtained in spring (2012/03, 2014/04) and summer (2010/07 and 2014/06) presented positive scores (Figure 8). Interestingly, N:Si and N:P contributed strongly to PC2 and both variables appeared strongly correlated with salinity. Contrastingly, the contribution of phosphate and silicate to PC2 was low, although these nutrients were positively correlated to PC1 (Figure 7). Most samples with positive scores for PC1 were collected below the Chl$_T$ *a* vertical maximum, with the exception of the samples collected during 2012/12 that had positive scores for PC1 and those obtained in 2015/04 which were poorly discriminated by this variance component. Therefore, it can be considered that PC1 represents the productivity gradient obtained from surface towards the lower limit of the euphotic layer. The fact that silicate and phosphate were negatively correlated to phytoplankton biomass as indicated by the PCA results (Figure 7) indicates that most of the variability in these nutrients was associated with the uptake by phytoplankton. Furthermore, the results of PCA permit the conclusion that Chl$_T$ *a* was apparently uncorrelated with salinity or temperature and weakly correlated to nitrate concentration. The third PC explained an important portion of variability (18%; Figure 7); salinity and phosphate contributed negatively to PC3 while S:P, silicate, N:P, and temperature did so positively. PC3 mainly discriminated between surveys, as most samples collected during the same survey had scores of the same sign. It is worth noting that all samples collected in 2014 and 2015 had negative scores for PC3.
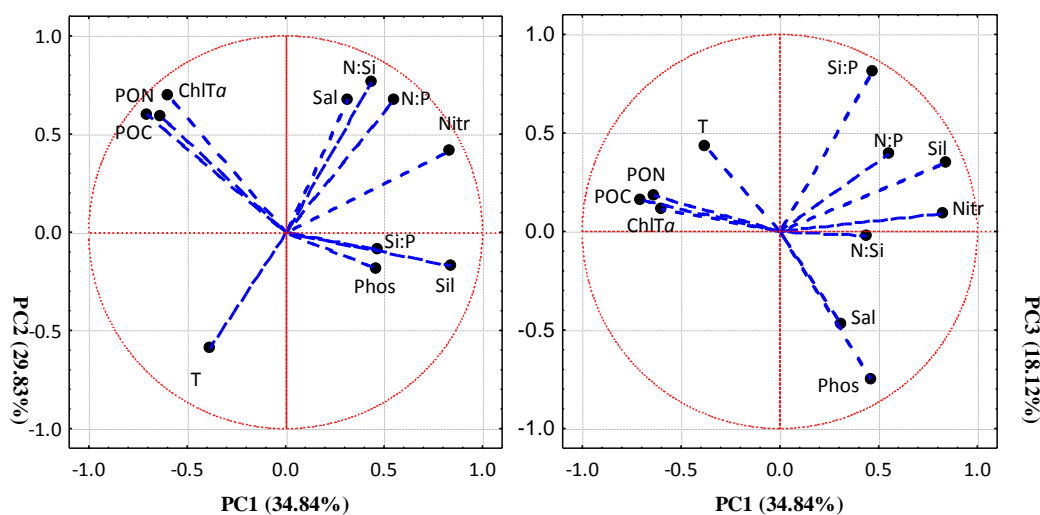

Figure 7. Vector-plots of the variable factor coordinates extracted from the principal component analysis (PCA); data coming from all samples collected in the euphotic layer were used. T, temperature; Sal, salinity; Nitr, nitrate; Phos, phosphate; Sil, silicate; N:P, molar ratio of nitrate+nitrite to phosphate; N:Si, molar ratio of nitrate+nitrite to silicate; Si:P, molar ratio of silicate to phosphate; ChlT*a*, total chlorophyll *a*; POC and PON, particulate organic carbon and nitrogen, respectively.
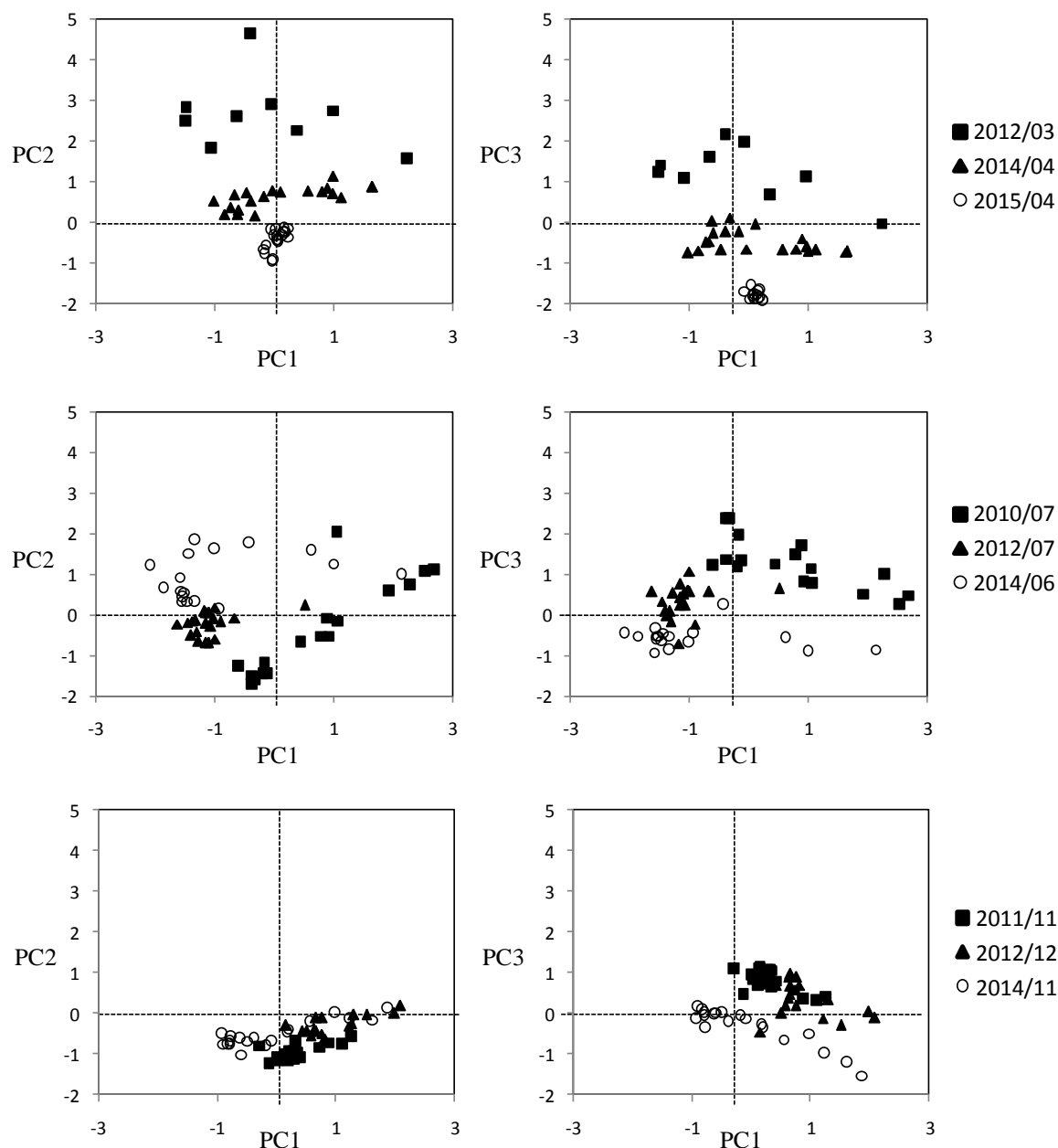
Figure 8. Bi-plot for the scores obtained for each sample for the three first principal components (PCs) extracted from the PCA (relation between PC1 and PC2, left panel,—and between PC1 and PC3, right panel). Data are grouped according to three seasonal periods: spring (**top**), summer (**middle**), and autumn (**bottom**).

3.4. Nutrient Discharges from Terrestrial Sources

The annual nutrient loads released from sewage point sources located at the north-western corner of the Alboran Sea for 2010–2015 are shown in Figure 9. Unfortunately, we have not found information regarding the exact location of these points; however, industry activity is concentrated in the northern coast of the BA and the population cores are distributed along the whole coast. These data preclude any quantitative analysis of the nutrient amount released into BA since they are aggregated with data from nearby coastal areas. However, some qualitative analyses can be made. Since the industrial activity in the northern Alboran Sea is mainly concentrated around the BA, it can be speculated that nitrate was the main source of inorganic nitrogen released from sewage during 2010–2015 (Figure 9). Furthermore, during that period, phosphate released from urban sewage varied substantially year to

year (note that industrial sewage did not contribute phosphate). Consequently, the N:P molar ratio in the sewage released into the BA would have varied from 400 in 2010 to less than 50 in 2013 (Figure 9). Tourism is not very intensive around the BA, and consequently the population and, by extension, the release of sewage is kept fairly stable during the year. Note that the nutrient inputs from river discharges have not been considered since annual loads of dissolved inorganic nitrogen and phosphate from the two main rivers into the BA are not available. It is also worth noting that these rivers are strongly dammed and consequently the freshwater flow is relatively low and depends mainly on the local rainfall regime, which is characterised by an annual drought period in summer (June, July and August). Nevertheless, according to the nutrient concentration measurements in the mouths of the two rivers (reported by the Andalusia Regional Government), it can be calculated that approximately 0.15 and 0.009 kt year^{-1} of nitrogen and phosphate are released within the BA during an annual period with a normal rainfall regime. These loads represent around 1% and 10% of the nitrate and phosphate, respectively, compared to the sewage loads shown in Figure 9. Regarding the non-point pollution sources, which release mainly nitrogen, the available data are also fairly scarce. In any case, according to [24], agriculture and livestock activity releases 0.47×10^{-3} kt year^{-1} of nitrogen towards the BA. This is about three magnitude orders or less than the nitrogen discharged from urban and industrial effluents.
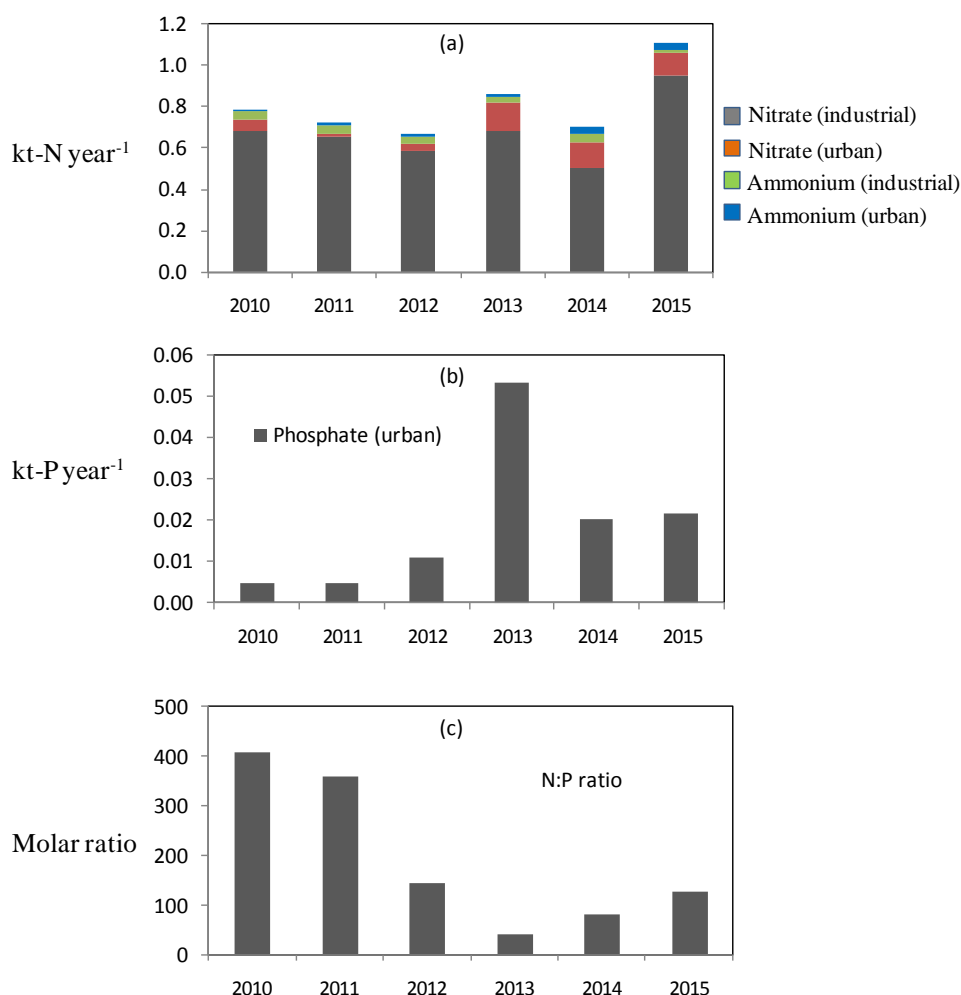

Figure 9. Loads of inorganic nitrogen (**a**) and phosphate (**b**) released from urban and industrial wastewaters in the north-western sector of the Alboran Sea. The N:P molar ratio in this effluent is also shown (**c**).

4. Discussion

Numerous studies have shown that physical and chemical features of the upper layer of the northern Alboran Sea are strongly conditioned by the dynamics of the AJ that penetrates throughout the Strait of Gibraltar [25,27]. Shifts in the position of the AJ relative to the shoreline, due to variations of the atmospheric pressure fields on both sides of the Strait of Gibraltar, produce modifications in the vertical position of the interface between SAW and MW that in turn favour (or disfavour) the upwelling of MW [27,28]. Wind regime is also important in regulating the AMI position as westerlies induce offshore Ekman transport and consequently promote MW upwelling in the continental shelf [20,25,27–32]. Both physical mechanisms have been also identified in the BA as drivers of the subinertial circulation patterns that, sequentially, regulate the position of the 37.5 isopycnal within the bay. According to Sánchez-Garrido et al. [13], when the AJ separates the northern shoreline, the circulation pattern of the surface water changes from anticyclonic to cyclonic. Additionally, easterlies tend to fill the bay with SAW and drain MW; while westerlies have the opposite effect. Obviously, these vertical displacements of the isopycnals are reflected in shifts of temperature and salinity in the surface layer, as shown by Sánchez-Garrido et al. [13]. Similarly, our analyses for the BA indicate that temperature and salinity variability among surveys in the euphotic layer, as well as the AMI vertical position, would be attributable to those mechanisms. A strong support for this statement is that the euphotic layer salinity averaged for each survey in the BA was strongly correlated with salinity in the other sampled area nearby, as expected if MW upwelling is fuelled by similar mechanisms in both areas. Additionally, on average, the euphotic layer salinity was higher and the AMI was shallower from March to May in the BA, as has been reported for other areas in the northern Alboran Sea [33]. Nevertheless, overall, salinity trended to be slightly higher in BA compared to ST, implying that certain local features of the BA would facilitate the mixing of SAW and MW. Among these features, tidal regime would play an important role as it also affects the exchange of SAW between inside and outside BA [14].

SAW and MW are distinguishable by presenting fairly different nutrient loads. SAW is usually nutrient-depleted, particularly in nitrate. Remineralisation processes occurring below the SAW layer lead to increased nutrient concentrations. In addition, the N:P molar ratios in the MW can reach values over 22:1, as compared to 16:1 in the SAW [27,34–38]. Consequently, in absence of other external nutrient sources, the supply of new nutrients towards the euphotic layer in the northern Alboran Sea relies strongly on the mechanisms that favour the MW upwelling. In fact, a tight relationship between MW upwelling intensity, nitrate and chlorophyll *a* concentration has been described in other northern coastal areas of the Alboran Sea [20,39–41]. However, according to the PCA results for the BA, the nutrient variability patterns were not clearly explained by changes in the circulation patterns of the water masses, as salinity and nutrient concentrations appeared weakly correlated. Thus, although higher values of N:Si and N:P ratios were related to higher salinity (as expected according to the differences in nutrient budget between SAW and MW), nitrate was weakly related to salinity, and silicate and phosphate appeared to vary independently of salinity. Furthermore, some samples collected during 2014 and 2015 showed high salinity and phosphate according to their scores for the third PC extracted from the PCA, but nitrate did not contribute to this variance component. A possible explanation for this weak correlation between nutrients and salinity is that nutrients were strongly impacted by phytoplankton consumption due to the expected relatively long residence time of the water masses within the Bay (10–20 days according to [14]). In fact, the PCA results indicate that Chl_T *a* was negatively correlated with silicate and phosphate. However, salinity is conservative and thus, a strong relationship between salinity and Chl_T *a* could be expected if high phytoplankton biomass is exclusively supported by upwelled nutrients. On the contrary, the PCA results indicate that Chl_T *a* varied regardless of salinity and temperature, and the correlation between both variables was not statistically significant ($n = 126$; $r^2 = 0.05$, $p > 0.05$). Interestingly, correlations between Chl_T *a* and salinity have also been described in other areas of the northern Alboran Sea such as the Bay of Malaga [42]. Therefore, our results suggest that the hydrological dynamics does not fully explain the variability in nutrient concentrations or chlorophyll *a* obtained during our research surveys.

An additional possible explanation for this weak relationship between MW upwelling indicators and nutrients is that nutrients released from land-based sources affected their concentration in the water column. Unfortunately, the lack of exhaustive inventories of sewage, river discharge, and non-point pollution sources within the BA means that a quantitative assessment of their impact at an adequate scale (comparable to our sampling time scale) cannot be made. However, the data shown in Figure 9 indicate that probably, at an annual scale, the main source of allochthonous inorganic nitrogen during 2010–2015 in the BA was nitrate, as the industrial activity in the northern Alboran Sea is centred in this area. Furthermore, during that period, phosphate delivered from urban sewage varied substantially year-to-year, and consequently the N:P molar ratio in the whole terrestrial inputs must be fairly variable. Note that the nitrate and phosphate inputs by river discharges and non-point sources are comparatively low as indicated by the calculations shown previously.

If we assume that the euphotic layer is normally occupied by SAW, the hypothetical impact of these pollution sources can be calculated considering the volume of SAW exchanged annually between outside and inside the BA, which was estimated by Sánchez-Garrido et al. [13] (Figure 10). Taking into account the nitrate and phosphate concentrations of the SAW that penetrates into the Alboran Sea through the Strait of Gibraltar [38], the annual exchange of nitrate and phosphate linked to SAW exchange is 11.4 and 1.2 kt year^{-1}, respectively. Nitrogen from sewage, river discharge, and non-point pollution sources would represent about 15%, 1.4% and less than 0.1% of the exchanged nitrate, respectively. Phosphate from sewage represents about 17% of exchange phosphate (note that the amount of phosphate from the other external sources is negligible). Therefore, on a yearly scale, nutrient budget in the euphotic layer of the BA can be significantly affected by nutrient release from land-based sources. However, at a lower time scale, the importance of these nutrient sources can become more or less reduced depending on the intensity of the MW upwelling. For instance, when the strong stratification of the water column hampers vertical mixing and consequently leads to depletion of nitrate in the euphotic layer, the release of nutrients from terrestrial sources should be more significant. These conditions normally occur during summer in the northern Alboran Sea [23,25,33]. The comparison between nutrient concentration in BA and ST during our summer surveys reveals that nitrate concentration in BA was substantially higher than in ST during 10/07 while phosphate followed the opposite pattern (Figure S2). Since salinity did not differ significantly between the two areas, it can be inferred that higher nitrate in BA was not related to more intensive MW upwelling. During 12/07 and 14/06, there were no significant differences in nitrate concentration between the two areas, however Chl$_T$ *a* was higher in the BA compared to ST, implying a higher nitrate availability for phytoplankton growth in the BA in summer. However, it cannot be discarded from our analysis that this poor correlation between nutrients and Chl$_T$ *a* also results from limitations of our sampling design. Firstly, the sample size is relatively reduced considering the space and time variability. Secondly, there is a lag period between the nutrient enrichment and the consequent increase of chlorophyll *a*. According to experiments carried out by Neale et al. [43] with communities collected in the Alboran Sea, an increase in diatom biomass (which is the group that more rapidly responds to nutrient enrichment) is produced within 24–48 h. The fact that diatom abundance was fairly reduced in 2010/07 despite nutrient concentration was high would indicate that the sampling was performed during this lag phase.

Other results indirectly support that extra-nitrate impacted its concentration within the BA. The means of nitrate and phosphate calculated for the euphotic layer during each survey were not correlated in the BA ($n = 9$; $r^2 = 0.08$; $p > 0.05$), while that correlation was significant in ST ($n = 7$; $r^2 = 0.71$, $p < 0.02$). Another possible indication of the impact of sewage nutrients in the BA is the fact that the samples collected in 2014 and 2015 were discriminated by the third variance component obtained from the PCA, mainly contributed by phosphate (negatively) and Si:P ratio (positively). The samples obtained during the mentioned period presented negative scores for PC3, indicating that phosphate concentrations trended to be higher than in the samples collected previously. It is worth noting that, coincidently, phosphate released from wastewater increased in 2013–215 compared to

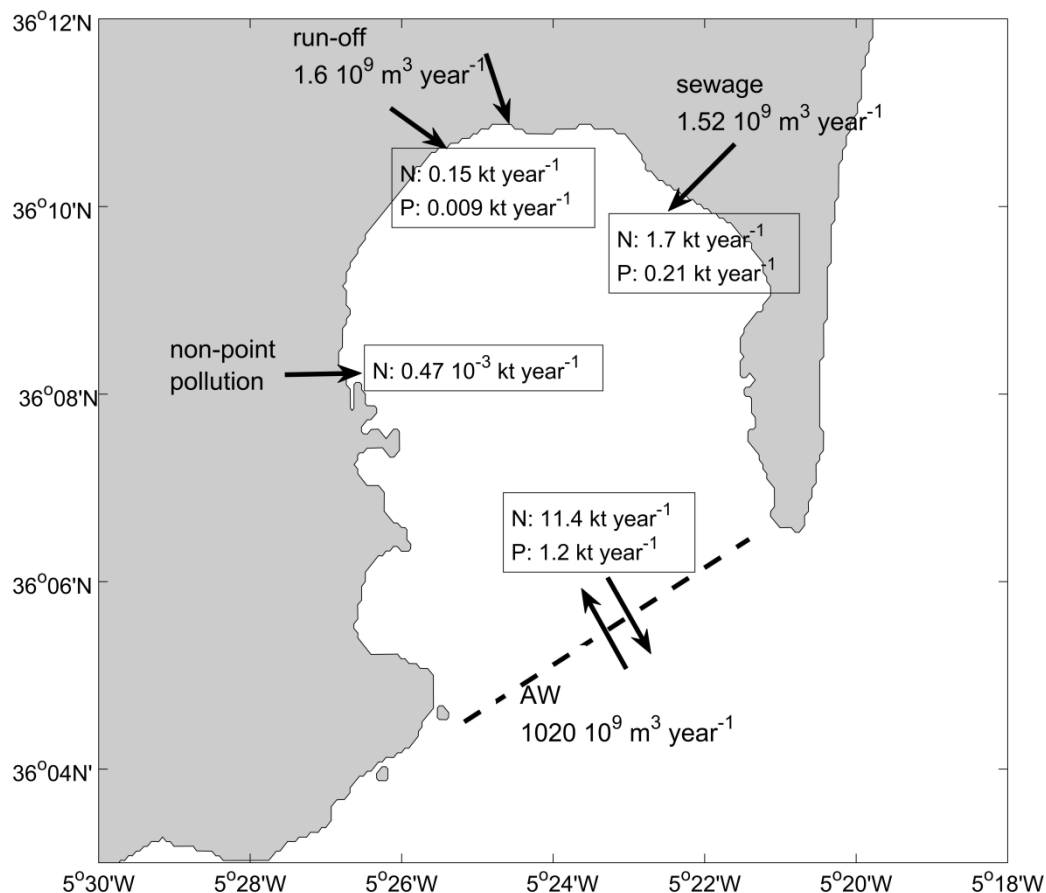2010–2012, which could be related to the growth of the population of the BA which occurred from 2012 onwards.

Figure 10. Estimation of yearly exchange of nitrate and phosphate between the outside and inside of the Bay of Algeciras (BA) associated to the Atlantic water flux (AW) and annual load of nitrogen and phosphorous from sewage, river discharge and non-point pollution sources. The overall amount of water associated to these sources (units: m^3 $year^{-1}$) is also shown (data from the non-point pollution not available).

In conclusion, our data indicate that the hydrological mechanisms that favour MW upwelling and the consequent nutrient enrichment of the euphotic layer within the BA are dealt with by drivers that act synchronically in other areas of the northern Alboran Sea. However, in contrast to those areas, the variability patterns in nutrient and chlorophyll *a* within the BA are not fully linked to these mechanisms, particularly in summer. In this period, the concentrations of nitrate and/or Chl_T *a* were higher than expected considering that the MW upwelling was disfavoured. A possible explanation for this poor correlation between hydrological features of the water column, nutrients, and chlorophyll *a* concentration is a significant impact of wastewater release in the BA. In particular, industrial effluents might be an additional source of nitrate. However, the evidence of the impact of these allochthonous nutrients is still indirect and more detailed data on sewage loads are necessary to establish more definitive conclusions. Furthermore, we cannot discard the potential influence of the limitations of our sampling design on the poor correlation between nutrients and Chl_T *a* observed in this study.

References

1. European Commission. Commission Decision of 1 September 2010 on criteria and methodological standards on good environmental status of marine waters (notified under document C(2010) 5956); (2010/477/EU)2010. *Off. J. Eur. Union* **2010**, *232*, 12–24.
2. Ferreira, J.G.; Jesper, H.; Andersen, J.H.; Borja, A.; Bricker, S.B.; Camp, J.; da Silva, M.C.; Garcés, E.; Heiskanen, A.S.; Humborg, C.; et al. Overview of eutrophication indicators to assess environmental status within the European Marine Strategy Framework Directive. *Estuar. Coast. Shelf Sci.* **2011**, *93*, 117–131. [CrossRef]
3. Harding, L.W.; Batiuk, R.A.; Fisher, T.R.; Gallegos, C.L.; Malone, T.C.; Miller, W.D.; Mulholland, M.R.; Paerl, H.W.; Perry, E.S.; Tango, P.J. Scientific bases for numerical chlorophyll criteria in Chesapeake Bay. *Estuaires Coasts* **2014**, *37*, 134–148. [CrossRef]
4. Cloern, J.E. Our evolving conceptual model of the coastal eutrophication problem. *Mar. Ecol. Prog. Ser.* **2001**, *210*, 223–253. [CrossRef]
5. McQuatters-Gollop, A.; Gilbert, A.J.; Mee, L.D.; Vermaat, J.E.; Artioli, Y.; Humborg, C.; Wulff, F. How well do ecosystem indicators communicate the effects of anthropogenic eutrophication? *Estuar. Coast. Shelf Sci.* **2009**, *82*, 583–596. [CrossRef]
6. Alpine, A.E.; Cloern, J.E. Trophic interactions and direct physical effects control phytoplankton biomass and production in an estuary. *Limnol. Oceanogr.* **1992**, *37*, 946–955. [CrossRef]
7. Balls, P.W.; Macdonald, A.; Pugh, K.; Edwards, A.C. Long-term nutrient enrichment of an estuarine system: Ythan, Scotland (1958-1993). *Environ. Pollut.* **1995**, *90*, 311–321. [CrossRef]
8. Pérez-Ruzafa, A.; Gilabert., J.; Gutiérrez, J.M.; Fernández, A.I.; Marcos, C.; Sabah, S. Evidence of a planktonic food web response to changes in nutrient input dynamics in the Mar Menor coastal lagoon, Spain. *Hydrobiologia* **2002**, *475/476*, 359–369.
9. Pérez-Ruzafa, A.; Fernández, A.I.; Marcos, C.; Gilabert, J.; Quispe, J.I.; García-Charton, J.A. Spatial and temporal variations of hydrological conditions, nutrients and chlorophyll *a* in a Mediterranean coastal lagoon (Mar Menor, Spain). *Hydrobiologia* **2005**, *550*, 11–27. [CrossRef]
10. Monbet, Y. Control of phytoplankton biomass in estuaries: A comparative analysis of microtidal and macrotidal estuaries. *Estuaries* **1992**, *15*, 563–571. [CrossRef]
11. Li, W.K.W.; Lewis, M.R.; Harrison, W.G. Multiscalarity of the nutrient–chlorophyll relationship in coastal phytoplankton. *Estuaries Coasts* **2010**, *33*, 440–447. [CrossRef]
12. Periáñez, R. Modelling the environmental behaviour of pollutants in Algeciras Bay (South Spain). *Mar. Pollut. Bull.* **2012**, *64*, 221–232. [CrossRef] [PubMed]
13. Sánchez-Garrido, J.C.; García-Lafuente, J.; Sammartino, S.; Naranjo, C.; de los Santos, F.J.; Álvarez-Fanjul, E. Meteorologically-driven circulation and flushing times of the Bay of Algeciras, Strait of Gibraltar. *Mar. Pollut. Bull.* **2014**, *80*, 94–106. [CrossRef] [PubMed]
14. Sammartino, S.; Sánchez-Garrido, J.C.; Naranjo, C.; García Lafuente, J.; Rodríguez Rubio, P.; Sotillo, M. Water renewal in semi-enclosed basins: A high resolution Lagrangian approach with application to the Bay of Algeciras, Strait of Gibraltar. *Limnol. Oceanogr. Methods* **2018**, *16*, 106–118. [CrossRef]

15. Morillo, J.; Usero, J.; El Bakouri, H. Biomonitoring of heavy metals in the coastal waters of two industrialised bays in southern Spain using the barnacle *Balanus amphitrite*. *Chem. Spec. Bioavailab.* **2008**, *20*, 227–237. [CrossRef]

16. Morales-Caselles, C.; Kalman, J.; Riba, I.; DelValls, T.A. Comparing sediment quality in Spanish littoral areas affected by acute (Prestige, 2002) and chronic (Bay of Algeciras) oil spills. *Environ. Pollut.* **2007**, *146*, 233–240. [CrossRef] [PubMed]

17. Sánchez-Moyano, J.E.; García-Adiego, E.M.; Estacio, F.; García-Gómez, J.C. Effect of environmental factors on the spatial variation of the epifaunal polychaetes of the alga *Halopteris scoparia* in Algeciras Bay (Strait of Gibraltar). *Hydrobiologia* **2002**, *470*, 133–148. [CrossRef]

18. Guerra-García, J.M.; Baeza-Rojano, E.; Cabezas, M.P.; Díaz-Pavón, J.J.; Pacios, I.; García-Gómez, J.C. The amphipods *Caprella penantis* and *Hyale schmidtii* as biomonitors of trace metal contamination in intertidal ecosystems of Algeciras Bay, Southern Spain. *Mar. Pollut. Bull.* **2009**, *58*, 765–786. [CrossRef] [PubMed]

19. Carballo, J.L.; Naranjo, S.A.; García, J.C. Use of marine sponges as stress indicators in marine ecosystems at Algeciras Bay (southern Iberian Peninsula). *Mar. Ecol. Prog. Ser.* **1996**, *135*, 109–122. [CrossRef]

20. Mercado, J.M.; Cortés, D.; García, A.; Ramírez, T. Seasonal and inter-annual changes in the planktonic communities of the northwest Alboran Sea (Mediterranean Sea). *Prog. Oceanogr.* **2007**, *74*, 273–293. [CrossRef]

21. Mercado, J.M.; Cortés, D.; Ramírez, T.; Gómez, F. Decadal weakening of the wind-induced upwelling reduces the impact of nutrient pollution in the Bay of Málaga (western Mediterranean Sea). *Hydrobiologia* **2012**, *680*, 91–107. [CrossRef]

22. Kara, A.B.; Rochford, P.A.; Hulbur, H.E. Efficient and accurate bulk parameterizations of air-sea fluxes for use in general circulation models. *J. Atmos. Ocean. Technol.* **2000**, *17*, 1421–1438. [CrossRef]

23. Mercado, J.M.; Ramírez, T.; Cortés, D.; Sebastián, M.; Liger, E.; Bautista, B. Partitioning the effects of changes in nitrate availability and phytoplankton community structure on the relative nitrate uptake in the Northwest Alboran Sea (Mediterranean Sea). *Mar. Ecol. Prog. Ser.* **2008**, *359*, 51–68. [CrossRef]

24. Consejería de Medio Ambiente y Ordenación del Territorio. *Memoria del Plan Hidrológico. Demarcación Hidrológica de las Cuencas Mediterráneas Andaluzas. Ciclo de Planificación Hidrológica 2015/2021*; Junta de Andalucía: Seville, Spain, 2016; 458p. (In Spanish)

25. Ramírez, T.; Cortés, D.; Mercado, J.M.; Vargas-Yañez, M.; Sebastián, M.; Liger, E. Seasonal dynamics of inorganic nutrients and phytoplankton biomass in the NW Alboran Sea. *Estuar. Coast. Shelf Sci.* **2005**, *65*, 654–670. [CrossRef]

26. Savenkoff, C.; Chanut, J.P.; Vezina, A.F.; Gratton, Y. Distribution of biological-activity in the lower St. Lawrence estuary as determined by multivariate analysis. *Estuar. Coast. Shelf Sci.* **1995**, *40*, 647–664. [CrossRef]

27. Minas, H.J.; Coste, B.; le Corre, P.; Minas, M.; Raimbault, P. Biological and geochemical signatures associated with the water circulation through the Strait of Gibraltar and in western Alboran Sea. *J. Geophys. Res.* **1991**, *96*, 8755–8771. [CrossRef]

28. Sarhan, T.; García-Lafuente, J.; Vargas, M.; Vargas, J.M.; Plaza, P. Upwelling mechanisms in the northwestern Alborán Sea. *J. Mar. Syst.* **2000**, *23*, 317–331. [CrossRef]

29. Tintoré, J.; Gomis, D.; Alonso, S.; Parrilla, G. Mesoscale dynamics and vertical motion in the Alboran Sea. *J. Phys. Oceanogr.* **1991**, *21*, 811–823. [CrossRef]

30. Macías, D.; Martin, A.P.; García-Lafuente, J.; García, X.M.; Yool, A.; Brun, M.; Vázquez, A.; Izquierdo, A.; Sein, D.; Echevarría, F. Mixing and biogeochemical effects induced by tides at on the Atlantic-Mediterranean flow in the Strait of Gibraltar. *Prog. Oceanogr.* **2007**, *74*, 252–272.

31. García-Górriz, E.; Carr, M.-E. Physical control of phytoplankton distributions in the Alboran Sea: A numerical and satellite approach. *J. Geophys. Res.* **2001**, *106*, 16795–16805. [CrossRef]

32. Gómez, F.; Gorsky, G.; Garcia-Gorriz, E.; Picheral, M. Control of phytoplankton distribution in the Strait of Gibraltar by wind and fortnightly tides. *Estuar. Coast. Shelf Sci.* **2004**, *59*, 85–497. [CrossRef]

33. Amorim, A.L.; León, P.; Mercado, J.M.; Cortés, D.; Gómez, F.; Putzeys, S.; Salles, S.; Yebra, L. Controls of picophytoplankton abundance and composition in a highly dynamic marine system, the Northern Alboran Sea (Western Mediterranean). *J. Sea Res.* **2016**, *112*, 13–22. [CrossRef]

34. Coste, B.; le Corre, P.; Minas, H.J. Re-evaluation of the nutrient exchanges in the Strait of Gibraltar. *Deep Sea Res. Part A* **1988**, *35*, 767–775. [CrossRef]

35.　Dafner, E.V.; Boscolo, R.; Bryden, H.L. The N:Si:P molar ratio in the Strait of Gibraltar. *Geophys. Res. Lett.* **2003**, *20*, 1506. [CrossRef]

36.　Gómez, F.; Gorsky, G.; Striby, L.; Vargas, J.M.; González, N.; Picheral, M.; García-Lafuente, J.; Varela, M.; Goutx, M. Small-scale temporal variations in biogeochemical features in the Strait of Gibraltar, Mediterranean side—The role of NACW and the interface oscillation. *J. Mar. Syst.* **2001**, *30*, 207–220. [CrossRef]

37.　Béthoux, J.P.; Morin, P.; Ruiz-Pino, D.P. Temporal trends in nutrient ratios: Chemical evidence of Mediterranean ecosystem changes driven by human activity. *Deep Sea Res. Part II Top. Stud. Oceanogr.* **2002**, *49*, 2007–2016. [CrossRef]

38.　Huertas, I.E.; Ríos, A.F.; García-Lafuente, J.; Navarro, G.; Makaoui, A.; Sánchez-Román, A.; Rodriguez-Galvez, S.; Orbi, A.; Ruíz, J.; Pérez, F.F. Atlantic forcing of the Mediterranean oligotrophy. *Glob. Biogeochem. Cycles* **2012**, *26*, GB2022. [CrossRef]

39.　Echevarría, F.; García-Lafuente, J.; Bruno, M.; Gorsky, G.; Goutx, M.; González, N.; García, C.M.; Gómez, F.; Vargas, J.M.; Picheral, M.; et al. Physical and biological coupling in the Strait of Gibraltar. *Deep Sea Res. Part II Top. Stud. Oceanogr.* **2002**, *49*, 4115–4130. [CrossRef]

40.　Reul, A.; Rodríguez, V.; Jiménez-Gómez, F.; Blanco, J.M.; Bautista, B.; Sarhan, T.; Guerrero, F.; Ruíz, J.; García-Lafuente, J. Variability in the spatio-temporal distribution and size–structure of phytoplankton across an upwelling area in the NW Alboran Sea (W-Mediterranean). *Cont. Shelf Res.* **2005**, *25*, 589–608. [CrossRef]

41.　Gómez, F.; González, N.; Echevarría, F.; García, C.M. Distribution and fluxes of dissolved nutrients in the Strait of Gibraltar and its relationships to microphytoplankton biomass. *Estuar. Coast. Shelf Sci.* **2000**, *51*, 439–449.

42.　Mercado, J.M.; Ramírez, D.; Cortés, D. Changes in nutrient concentration induced by hydrological variability and its effects on light absorption by phytoplankton in the Alboran Sea (Western Mediterranean Sea). *J. Mar. Syst.* **2008**, *71*, 31–45. [CrossRef]

43.　Neale, P.J.; Sobrino, C.; Segovia, M.; Mercado, J.M.; León, P.; Cortés, D.; Tuite, P.; Picazo, A.; Salles, S.; Cabrerizo, M.J.; Prasil, O. Effects of CO_2, nutrients and light on coastal plankton. I. Abiotic conditions and biological responses. *Aquat. Biol.* **2014**, *22*, 25–41. [CrossRef]